Binary Radio Pulsars
ASP Conference Series, Vol. 328, 2005
F. A. Rasio and I. H. Stairs

Overview of Pulsar Tests of General Relativity

Ingrid Stairs

Dept. of Physics and Astronomy, University of British Columbia, 6224 Agricultural Road, Vancouver, B.C. V6T 1Z1, Canada

Abstract. Radio pulsar observations can be used to test aspects of general relativity from equivalence principle violations to binary orbital effects in the strong-field regime. This article summarizes the status of such tests at the start of the meeting, and describes two new tests made possible by recent observations of well-known binary pulsar systems.

1. Introduction

The potential of pulsars for high-precision tests of the predictions of general relativity (GR) was recognized immediately upon the discovery of the first pulsar binary system, PSR B1913+16 (Hulse & Taylor 1975, Wagoner 1975, Eardley 1975, Damour & Ruffini 1974, Barker & O'Connell 1975a,b). Since then, pulsars have provided stringent tests of equivalence principle violations and both radiative and quasi-static strong-field effects. This article presents an overview of these tests (see also Stairs 2003 for a fuller description of much of this material) and a snapshot of the results as of the start of this meeting. Further details on and updates of some of the tests discussed below can be found in other articles (Lorimer & Freire; Bailes; Weisberg & Taylor) in this volume, and the double-pulsar system is the subject of numerous other articles and will not be discussed in detail here.

2. Equivalence Principle Violations

Equivalence principles describe our expectations of experimental outcomes in different reference frames. The Weak Equivalence Principle (WEP), formulated by Newton, states that in an external gravitational field, objects of different compositions and masses will experience the same acceleration. The Einstein Equivalence Principle (EEP) extends this idea to include Lorentz invariance (non-existence of preferred reference frames) and positional invariance (non-existence of preferred locations) for non-gravitational experiments, predicting that these experiments will have the same outcomes in inertial and in freely-falling reference frames. The Strong Equivalence Principle (SEP) adds Lorentz and positional invariance for gravitational experiments, thus including experiments on objects with strong self-gravitation. GR incorporates the SEP, but alternate theories of gravity may violate all or parts of it.

The parametrized post-Newtonian (PPN) formalism (Will & Nordvedt 1972) provides a uniform description of the weak-gravitational-field limit and facilitates comparisons of different gravitational theories theories in this limit. This formalism has 10 parameters ($\gamma_{\rm PPN}$, β, ξ,α_1, α_2, α_3, ζ_1, ζ_2, ζ_3 and ζ_4); see Will (2001) for full descriptions and physical meanings of these parameters. Damour and Esposito-Farèse (1992b, 1996a) extended this formalism to include strong-field effects for generalized tensor-multiscalar gravitational theories. This allows a better understanding of limits in the strong-field regime imposed by systems including pulsars and white dwarfs, for which the amounts of self-gravitation are very different. Here, for instance, α_1 becomes $\hat{\alpha_1} = \alpha_1 + \alpha_1'(c_1 + c_2) + ...$, where c_i describes the "compactness" of mass m_i . The compactness can be written $c_i = -2\partial \ln m_i/\partial \ln G \simeq -2(E^{\rm grav}/(mc^2))_i$, where G is Newton's constant and $E_i^{\rm grav}$ is the gravitational self-energy of mass m_i. The compactness is about -0.2 for a neutron star (NS) and -10^{-4} for a white dwarf (WD). Pulsar timing sets limits on $\hat{\alpha_1}$, which tests for the existence of preferred-frame effects (violations of Lorentz invariance) and $\hat{\alpha}_3$, which, in addition to testing for preferred-frame effects, also implies non-conservation of momentum if non-zero. (A test of $\hat{\zeta}_2$, which is also a non-conservative parameter, relies on the second period derivative of the double-neutron-star binary PSR B1913+16 (Will 1992). As a measurement of this quantity could also be due to timing noise or to geodetic precession (Konacki, Wolszczan & Stairs 2003) this test will not be considered further.) Pulsars can also be used to set limits on other SEP-violation effects which constrain combinations of the PPN parameters: the Nordtvedt ("gravitational Stark") effect, dipolar gravitational radiation, and variation of Newton's constant.

2.1. Strong Equivalence Principle

Nordvedt (1968) first suggested direct tests of the SEP through Lunar Laser Ranging (LLR) experiments. As the masses of Earth and the Moon contain different fractional contributions from self-gravitation, a violation of the SEP would cause them to fall differently in the Sun's gravitational field and "polarize" the orbit in the direction of the Sun. LLR tests have set a limit of $|\eta| < 0.001$ (e.g., Dickey et al. 1994; Will 2001), where η is a combination of PPN parameters:

$$\eta = 4\beta - \gamma - 3 - \frac{10}{3}\xi - \alpha_1 + \frac{2}{3}\alpha_2 - \frac{2}{3}\zeta_1 - \frac{1}{3}\zeta_2. \quad (1)$$

The strong-field formalism uses the parameter $\Delta_{\rm i}$ (Damour & Schäfer 1991), which allows for non-linear dependence on the compactness and which for object "i" may be written as:

$$\begin{aligned} \left(\frac{m_{\rm grav}}{m_{\rm inertial}}\right)_i &= 1 + \Delta_{\rm i} \\ &= 1 + \eta\left(\frac{E^{\rm grav}}{mc^2}\right)_i + \eta'\left(\frac{E^{\rm grav}}{mc^2}\right)_i^2 + \ldots. \end{aligned} \quad (2)$$

Pulsar–white dwarf systems constrain the difference $\Delta_{\rm net} = \Delta_{\rm pulsar} - \Delta_{\rm companion}$ (Damour & Schäfer 1991). If the SEP is violated, the equations of motion for

such a system will contain an extra acceleration $\Delta_{\rm net}\mathbf{g}$, where $\mathbf{g}$ is the gravitational acceleration due to the Galaxy. This term will influence the evolution of the orbit of the system. For low-eccentricity orbits, the largest effect will be to force the eccentricity toward alignment with the projection of $\mathbf{g}$ onto the orbital plane of the system. Therefore the time evolution of the eccentricity vector will not only depend on the usual GR-predicted relativistic advance of periastron ($\dot{\omega}$) but will also include a constant term. Damour and Schäfer (1991) write the time-dependent eccentricity vector as:

$$\mathbf{e}(t) = \mathbf{e}_F + \mathbf{e}_R(t), \tag{3}$$

where $\mathbf{e}_R(t)$ is the $\dot{\omega}$-induced rotating eccentricity vector, and $\mathbf{e}_F$ is the forced component. In terms of $\Delta_{\rm net}$, the magnitude of $\mathbf{e}_F$ is (Damour & Schäfer 1991; Wex 1997):

$$|\mathbf{e}_F| = \frac{3}{2}\frac{\Delta_{\rm net}\mathbf{g}_\perp}{\dot{\omega}a(2\pi/P_{\rm b})}, \tag{4}$$

where $\mathbf{g}_\perp$ is the projection of the gravitational field onto the orbital plane, and $a = x/(\sin i)$ is the semi-major axis of the orbit. For small-eccentricity systems, this becomes:

$$|\mathbf{e}_F| = \frac{1}{2}\frac{\Delta_{\rm net}\mathbf{g}_\perp c^2}{FG\,M(2\pi/P_{\rm b})^2}, \tag{5}$$

where M is the total mass of the system, and, in GR, $F = 1$ and G is Newton's constant.

The primary criterion for selecting pulsars to test the SEP is for the orbital system to have a large value of $P_{\rm b}^2/e$, greater than or equal to 10^7 days^2 (Wex 1997). However, as pointed out by Damour and Schäfer (1991) and Wex (1997) (see also Lorimer & Freire, in this volume), two age-related restrictions are also needed. First, the pulsar must be sufficiently old that the $\dot{\omega}$-induced rotation of $\mathbf{e}$ has completed many turns and $\mathbf{e}_R(t)$ can be assumed to be randomly oriented. This requires that the characteristic age $\tau_{\rm c} \gg 2\pi/\dot{\omega}$. Secondly, $\dot{\omega}$ itself must be larger than the rate of Galactic rotation, so that the projection of $\mathbf{g}$ onto the orbit can be assumed to be constant. According to Wex (1997), this holds true for pulsars with orbital periods of less than about 1000 days.

Obtaining a limit on $\Delta_{\rm net}$ requires statistical averages over the unknowns in the problem. To account for the random orientation of $\mathbf{e}_R$, Wex (1997, 2000) uses the inequality:

$$|\mathbf{e}_F| \le e\xi_1(\theta), \quad \xi_1(\theta) = \left[\begin{array}{rcl} 1/\sin\theta & : & \theta \in [0, \pi/2) \\ 1 & : & \theta \in [\pi/2, 3\pi/2] \\ -1/\sin\theta & : & \theta \in (3\pi/2, 2\pi) \end{array}\right. , \tag{6}$$

where $e = |\mathbf{e}|$, and θ (the angle between $-\mathbf{g}_\perp$ and $\mathbf{e}_R$; see Figure 1 and Damour & Schäfer 1991) is assumed to have a uniform probability distribution between 0 and 2π.

The projection of $\mathbf{g}$ onto the orbital plane can be written:

$$|\mathbf{g}_\perp| = |\mathbf{g}|[1 - (\cos i\cos\lambda + \sin i\sin\lambda\sin(\phi - \Omega))^2]^{1/2}, \tag{7}$$

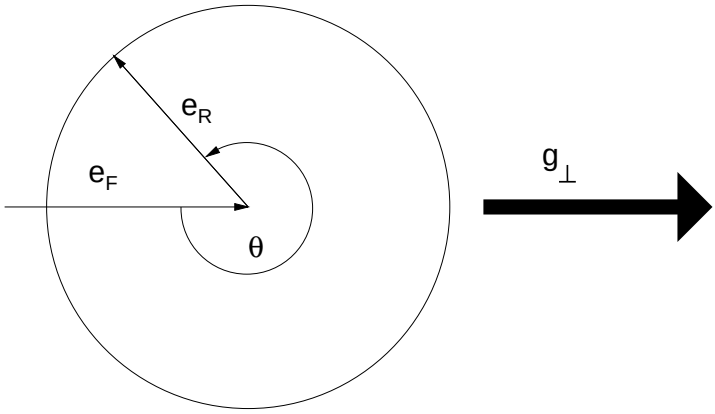

Figure 1. "Polarization" of a nearly circular binary orbit under the influence of a forcing vector $\mathbf{g}$, showing the relation between the forced eccentricity, $\mathbf{e}_F$, the eccentricity evolving under the general-relativistic advance of periastron, $\mathbf{e}_R(t)$, and the angle θ. After Wex (1997).

where i in the inclination angle of the orbital plane relative to the line of sight, ϕ is the position angle of the projection of the gravitational acceleration vector $\mathbf{g}$ onto the plane of the sky, Ω is the position angle of the line of nodes and λ is the angle between the line from pulsar to Earth and $\mathbf{g}$ (Damour & Schäfer 1991). The values of λ and $|\mathbf{g}|$ can be determined from geometry and models of the Galactic potential (e.g., Kuijken & Gilmore 1989), respectively. The inclination angle i can be estimated if even crude estimates of the neutron star and companion masses are available, from statistics of NS masses (e.g., Thorsett & Chakrabarty 1999) and/or the core-mass–orbital-period relation between the size of the orbit and the WD companion mass (e.g., Rappaport et al. 1995). However, the angle Ω is also usually unknown and must also be assumed to be uniformly distributed between 0 and 2π.

Damour and Schäfer (1991) use the PSR B1953+29 system (which had the largest value of $P_{\rm b}^2/e$ known at the time) and integrate over the angles θ and Ω to determine a 90% confidence upper limit of $\Delta_{\rm net} < 1.1 \times 10^{-2}$. Wex (1997) takes an ensemble of pulsars, calculating for each system the probability (fractional area in θ–Ω space) that $\Delta_{\rm net}$ is less than a given value, and then deriving an overall probability for each value of $\Delta_{\rm net}$. In this way he derives $\Delta_{\rm net} < 5 \times 10^{-3}$ at 95% confidence. An updated version of this calculation is presented by Lorimer & Freire (in this volume). In an attempt to account for possible selection effects, Wex (2000) tackles the problem from the other direction. Given a value of $\Delta_{\rm net}$, an upper limit on $|\theta|$ is obtained from equation 6. A Monte Carlo simulation of the expected pulsar population (assuming a range of masses based on evolutionary models and a random orientation of Ω) then yields a certain fraction of the population that agree with this limit on $|\theta|$. The collection of

pulsars ultimately gives a limit of $\Delta_{\rm net} < 9\times10^{-3}$ at 95% confidence, a somewhat weaker limit.

A qualitative improvement to the test can be made using PSR J1713+0737, using the fact that the full orientation of its orbit (i.e., the parameters i and Ω), as well as the two stellar masses and the parallax, are now known to within small uncertainties from high-precision pulse timing (Splaver et al. 2005). This means fewer statistical averages are needed for this system. Through a Monte-Carlo simulation in which the (covariant) uncertainty ranges are thoroughly sampled and θ is still assumed to be randomly distributed, a limit of $|\Delta_{\rm net}| < 0.013$ (95% confidence) is derived. While not as stringent as the limit derived from an ensemble of pulsars, it is nonetheless important as it is a unique type of limit.

2.2. $\hat{\alpha}_1$ and $\hat{\alpha}_3$

A non-zero $\hat{\alpha_1}$ (the strong-field analog of α_1) implies that the velocity $\mathbf{w}$ of a pulsar system (relative to a "universal" background reference frame given by the Cosmic Microwave Background, or CMB) will affect its orbital evolution, forcing the eccentricity to align with the projection of the system velocity onto the orbital plane.

The analysis proceeds in a similar fashion to that for $\Delta_{\rm net}$, except that the magnitude of $\mathbf{e}_F$ is now written as (Damour & Esposito-Farèse 1992a; Bell, Camilo, & Damour 1996):

$$|\mathbf{e}_F| = \frac{1}{12}\hat{\alpha_1}\left|\frac{m_1-m_2}{m_1+m_2}\right|\frac{|\mathbf{w}_\perp|}{[G(m_1+m_2)(2\pi/P_{\rm b})]^{1/3}}, \tag{8}$$

where $\mathbf{w}_\perp$ is the projection of the system velocity onto the orbital plane. The angle λ, used in determining this projection in a manner similar to that of equation 7, is now the angle between the line of sight to the pulsar and the absolute velocity of the binary system, and ϕ is now the angle of the projection of the absolute velocity vector onto the plane of the sky.

The figure of merit for systems used to test $\hat{\alpha_1}$ is $P_{\rm b}^{1/3}/e$. The same age requirements apply as for the $\Delta_{\rm net}$ test. Examples of suitable systems are PSR J2317+1439 (Camilo, Nice, & Taylor 1993; Bell, Camilo, & Damour 1996) with a last published value of $e < 1.2\times10^{-6}$ in 1996 (Camilo et al. 1996), and PSR J1012+5307, with $e < 8\times10^{-7}$ (Lange et al. 2001). This latter system is especially valuable because observations of its white-dwarf component yield a radial velocity measurement (Callanan, Garnavich, & Koester 1998) eliminating the need to take into account a range of possible values for the radial velocity. The analysis of Wex (2000) yields a limit of $\hat{\alpha_1} < 1.4\times10^{-4}$. This is comparable in magnitude to the weak-field results from lunar laser ranging, but incorporates strong field effects as well.

Tests of $\hat{\alpha}_3$ can be derived from both binary and single pulsars. A non-zero $\hat{\alpha}_3$, which implies both a violation of local Lorentz invariance and non-conservation of momentum, will cause a rotating body to experience a self-acceleration $\mathbf{a}_{\rm self}$ in a direction orthogonal to both its spin $\mathbf{\Omega}_{\rm Sp}$ and its absolute velocity $\mathbf{w}$

(Nordtvedt & Will 1972):

$$\mathbf{a}_{\rm self} = -\frac{1}{3}\hat{\alpha}_3 \frac{E^{\rm grav}}{(m\,c^2)}\mathbf{w} \times \mathbf{\Omega}_{\rm Sp}. \tag{9}$$

Thus the self-acceleration depends strongly on the compactness of the object.

An ensemble of isolated pulsars can be used to set a limit on $\hat{\alpha}_3$ as follows. For any given pulsar, it is likely that some fraction of the self-acceleration will be directed along the line of sight to the Earth. Such an acceleration will contribute to the observed period derivative $\dot{P}$ via the Doppler effect, by an amount:

$$\dot{P}_{\hat{\alpha}_3} = \frac{P}{c}\hat{\mathbf{n}} \cdot \mathbf{a}_{\rm self}, \tag{10}$$

where $\hat{\mathbf{n}}$ is a unit vector in the direction to the pulsar from the Earth. Will (1993) assumes random orientations of both the pulsar spin axes and velocities, and finds that, on average, $|\dot{P}_{\hat{\alpha}_3}| \simeq 5\times10^{-5}|\hat{\alpha}_3|$, independent of the pulse period. The *sign* of the $\hat{\alpha}_3$ contribution to $\dot{P}$, however, may be positive or negative for any individual pulsar, thus if there were a large contribution on average, one would expect to observe pulsars with both positive and negative total period derivatives. Young pulsars in the field of the Galaxy all show positive period derivatives, typically around 10^{-14}s/s. Thus the maximum possible contribution from $\hat{\alpha}_3$ must also be considered to be of this size, and the limit is given by $|\hat{\alpha}_3| < 2\times10^{-10}$ (Will 1993). Bell (1996) applies this test to a set of millisecond pulsars, which have much smaller period derivatives, on the order of 10^{-20}s/s. Here it is also necessary to account for the "Shklovskii effect" (Shklovskii 1970) in which a similar (always positive) Doppler-shift addition to the period derivative results from the transverse motion of the pulsar on the sky. Once this correction is applied to the observed period derivatives for isolated millisecond pulsars, a limit on $|\hat{\alpha}_3|$ on the order of 10^{-15} results (Bell 1996; Bell & Damour 1996).

In the case of a binary pulsar–white-dwarf system, both bodies experience a self-acceleration. The most important effect is a coupling of the spins to the absolute motion of the centre of mass. Both the compactness and the spin of the pulsar will completely dominate those of the white dwarf, making the net acceleration of the two bodies effectively (Bell & Damour 1996):

$$\mathbf{a}_{\rm self} = \frac{1}{6}\hat{\alpha}_3 c_{\rm p}\mathbf{w} \times \mathbf{\Omega}_{\rm Sp}, \tag{11}$$

where $c_{\rm p}$ and $\mathbf{\Omega}_{\rm Sp}$ denote the compactness and spin angular frequency of the pulsar, respectively, and $\mathbf{w}$ is the velocity of the system. On evolutionary grounds (e.g., Bhattacharya & van den Heuvel 1991), the spin axis of the pulsar may be assumed to be aligned with the orbital angular momentum of the system, hence the net effect of the acceleration will be, once again, to induce a polarization of the eccentricity vector within the orbital plane. The forced eccentricity term may be written as:

$$|\mathbf{e}_F| = \hat{\alpha}_3 \frac{c_{\rm p}|\mathbf{w}|}{24\pi}\frac{P_{\rm b}^2}{P}\frac{c^2}{G(m_1+m_2)}\sin\beta \tag{12}$$

where β is the (unknown) angle between $\mathbf{w}$ and $\mathbf{\Omega}_{\rm Sp}$, and P is, as usual, the spin period of the pulsar: $P = 2\pi/\Omega_{\rm Sp}$.

The figure of merit for systems used to test $\hat{\alpha}_3$ is $P_{\rm b}^2/(eP)$. The additional requirements of $\tau_{\rm c} \gg 2\pi/\dot{\omega}$ and $\dot{\omega}$ being larger than the rate of Galactic rotation also hold. The 95% confidence limit derived by Wex (2000) for an ensemble of binary pulsars is $|\hat{\alpha}_3| < 1.5 \times 10^{-19}$, much more stringent than for the single-pulsar case.

Again, PSR J1713+0747 allows a new type of limit due to the measurement of the orientation of its orbit (Splaver et al. 2005). Sampling the full range of allowed angular, mass and distance parameters, and finding the "worst case" radial velocity for each trial system, a limit of $|\hat{\alpha}_3| < 1.2 \times 10^{-19}$ is found, even stronger than that derived from the ensemble of pulsars, and less statistical in nature.

3. Dipolar Gravitational Radiation

General Relativity predicts gravitational radiation from the time-varying mass quadrupole of a binary pulsar system, but does *not* predict *dipolar* gravitational radiation, though many theories that violate the SEP do. In these theories, dipolar gravitational radiation results from the difference in gravitational binding energy of the two components of a binary. For this reason, neutron star–white dwarf binaries are the ideal laboratories to test the strength of such dipolar emission. The expected rate of change of the period of a circular orbit due to dipolar emission can be written as (Will 1993; Damour & Esposito-Farèse 1996b):

$$\dot{P}_{\rm b\,Dipole} = -\frac{4\pi^2 G_*}{c^3\, P_{\rm b}} \frac{m_1 m_2}{m_1 + m_2} (\alpha_{c_1} - \alpha_{c_2})^2, \tag{13}$$

where $G_* = G$ in GR, and α_{c_i} is the coupling strength of body "i" to a scalar gravitational field (Damour & Esposito-Farèse 1996b). The best test systems here are of course pulsar–white dwarf binaries with short orbital periods, such as PSRs B0655+64 and J1012+5307 (both with circular orbits) and the eccentric PSR J1141−6545. In these cases, $\alpha_{c_1} \gg \alpha_{c_2}$ so that a strong limit can be set on the coupling of the pulsar itself. The most recent limit for PSR B0655+64 comes from Arzoumanian (2003), who sets a 2-σ upper limit of $|\dot{P}_{\rm b}/P_{\rm b}| < 1 \times 10^{-10}\,{\rm yr}^{-1}$, or $|\dot{P}_{\rm b}| < 2.7 \times 10^{-13}$, which yields $(\alpha_{c_1} - \alpha_0)^2 < 2.7 \times 10^{-4}$, where α_0 is a reference value of the coupling at infinity. For PSR J1012+5307, a Shklovskii correction (Shklovskii 1970) for the transverse motion of the system and a correction for the (small) predicted amount of quadrupolar radiation must first be subtracted from the observed upper limit to arrive at $\dot{P}_{\rm b} = (-0.6 \pm 1.1) \times 10^{-13}$ and $(\alpha_{c_1} - \alpha_0)^2 < 4 \times 10^{-4}$ at 95% confidence (Lange et al. 2001). It should be noted that both these limits depend on estimates of the masses of the two stars and do not address the (unknown) equation of state of the neutron stars.

The young-pulsar–white-dwarf system PSR J1141−6545 (Kaspi et al. 2000) is eccentric and therefore expected to emit large amounts of quadrupolar gravitational radiation. The resulting orbital period derivative has recently been measured (Bailes et al. 2003; see also Bailes, in this volume) and found to be in

good agreement with the predictions of GR, thus this system can also be used to exclude dipolar radiation (Gerard & Wiaux 2002) and to set even stronger limits on tensor-scalar theories than the circular-orbit systems (Esposito-Farèse 2003). It currently sets a limit of $(\alpha_{c_1} - \alpha_0)^2 < 1.3 \times 10^{-4}$, and this should improve dramatically as the measurement on $\dot{P}_\mathrm{b}$ improves (Esposito-Farèse 2003).

Limits may also be derived from double-neutron-star systems (e.g., Will 1977; Will & Zaglauer 1989), although here the difference in the coupling constants is small and so the expected amount of dipolar radiation is also small compared to the quadrupole emission. However, certain alternative gravitational theories in which the quadrupolar radiation predicts a *positive* orbital period derivative independently of the strength of the dipolar term (e.g., Rosen 1973; Ni 1973; Lightman & Lee 1973) are ruled out by the observed decreasing orbital period in these systems (Weisberg & Taylor 1981).

4. Variation of Newton's Constant

Theories that violate the SEP by allowing for preferred space-time locations may permit Newton's constant, G, to vary. In general, variations in G are expected to occur on the timescale of the age of the Universe, such that $\dot{G}/G \sim H_0 \sim 0.7 \times 10^{-10}\,\mathrm{yr}^{-1}$, where H_0 is the Hubble constant. Three different pulsar-derived tests can be applied to these predictions, as a SEP-violating time-variable G would be expected to alter the properties of neutron stars and white dwarfs, and to affect binary orbits.

By changing the gravitational binding energy of neutron stars, a non-zero $\dot{G}$ would reasonably be expected to alter the moment of inertia of the star and so change its spin on the same timescale (Counselman & Shapiro 1968). Goldman (1990) writes:

$$\left(\frac{\dot{P}}{P}\right)_{\dot{G}} = \left(\frac{\partial \ln I}{\partial \ln G}\right)_N \frac{\dot{G}}{G}, \tag{14}$$

where I is the moment of inertia of the neutron star, about $10^{45}\,\mathrm{g\,cm}^2$, and N is the (conserved) total number of baryons in the star. By assuming that this represents the *only* contribution to the observed $\dot{P}$ of PSR B0655+64, in a manner similar to the isolated-pulsar test of $\hat{\alpha}_3$ described above, Goldman then derives an upper limit of $|\dot{G}/G| \leq (2.2 - 5.5) \times 10^{-11}\,\mathrm{yr}^{-1}$, depending on the stiffness of the neutron star equation of state. Arzoumanian (1995) applies similar reasoning to PSR J2019+2425 (Nice, Taylor, & Fruchter 1993) which has a characteristic age of 27 Gyr once the "Shklovskii" correction is applied (Nice & Taylor 1995). Again depending on the equation of state, the upper limits from this pulsar are $|\dot{G}/G| \leq (1.4 - 3.2) \times 10^{-11}\,\mathrm{yr}^{-1}$ (Arzoumanian 1995). These values are similar to those obtained by solar-system experiments such as radar ranging to the Viking Lander on Mars (e.g., Reasenberg 1983). Several other millisecond pulsars, once "Shklovskii" and Galactic-acceleration corrections are taken into account, have similarly large characteristic ages (e.g. Camilo et al. 1996, Toscano et al. 1996). The quality of this test, of course, depends on the reliability of the characteristic age as a measure of the true pulsar age.

In a binary system, a varying G will affect the individual stars and the total mass and angular momentum of the binary system, causing an orbital period derivative that may be written as (Damour, Gibbons, & Taylor 1988; Nordtvedt 1990):

$$\left(\frac{\dot{P}_{\rm b}}{P_{\rm b}}\right)_{\dot{G}} = -\left[2 - \left(\frac{m_1 c_1 + m_2 c_2}{m_1 + m_2}\right) - \frac{3}{2}\left(\frac{m_1 c_2 + m_2 c_1}{m_1 + m_2}\right)\right]\frac{\dot{G}}{G}. \qquad (15)$$

The best limit comes from the neutron-star–white dwarf system PSR B1855+09, with a measured limit on $\dot{P}_{\rm b}$ of $(0.6 \pm 1.2) \times 10^{-12}$ (Kaspi, Taylor, & Ryba 1994; Arzoumanian 1995); this leads to a bound of $\dot{G}/G = (-1.3 \pm 2.7) \times 10^{-11}\,{\rm yr}^{-1}$. Prospects for improvement come directly from improvements to the limit on $\dot{P}_{\rm b}$. Even though PSR J1012+5307 has a tighter limit on $\dot{P}_{\rm b}$ (Lange et al. 2001), its shorter orbital period means that the $\dot{G}$ limit it sets is a factor of 2 weaker than for PSR B1855+09. Recent timing of PSR J1713+0747 (Splaver et al. 2005) should allow a tighter limit.

The Chandrasekhar mass, $M_{\rm CH}$, is the maximum mass possible for a white dwarf supported against gravitational collapse by electron degeneracy pressure (Chandrasekhar 1931). Its value — about $1.4\,M_\odot$ — depends on Newton's constant: $M_{\rm CH} \sim (\hbar\, c/G)^{3/2}/m_{\rm N}^2$, where $\hbar$ is Planck's constant and $m_{\rm N}$ is the neutron mass. The majority of measured and constrained pulsar masses are consistent with a narrow distribution centred very close to $M_{\rm CH}$: $1.35 \pm 0.04\,M_\odot$ (Thorsett & Chakrabarty 1999,but see the article by Nice et al., in this volume). Thus it is reasonable to assume that $M_{\rm CH}$ sets the typical neutron star mass, and to check for any changes in the average neutron star mass over the lifetime of the Universe. Thorsett (1996) compiles a list of measured and average masses from 5 double-neutron-star binaries with ages ranging from 0.1 Gyr to 12 or 13 Gyr in the case of the globular-cluster binary B2127+11C. Using a Bayesian analysis, he finds a limit of $\dot{G}/G = (-0.6 \pm 4.2) \times 10^{-12}\,{\rm yr}^{-1}$ at the 95% confidence level.

5. Strong-Field Gravity

The best-known uses of pulsars for testing the predictions of gravitational theories are those in which the predicted strong-field effects are compared directly against observations. As essentially point-like objects in strong gravitational fields, neutron stars in binary systems provide extraordinarily clean tests of these predictions.

In any given theory of gravity, the post-Keplerian (PK) parameters (advance of periastrion $\dot{\omega}$, orbital period derivative $\dot{P}_{\rm b}$, time dilation/gravitational redshift γ and range r and shape s of Shapiro delay) can be written as functions of the pulsar and companion star masses and the Keplerian parameters if spin-orbit contributions can be neglected. As the two stellar masses are the only unknowns in the description of the orbit, it follows that measurement of any two PK parameters will yield the two masses, and that measurement of three or more PK parameters will over-determine the problem and allow for self-consistency checks. It is this test for internal consistency among the PK parameters that forms the basis of the classic tests of strong-field gravity. It should be noted that

the basic Keplerian orbital parameters are well-measured and can effectively be treated as having negligible uncertainties.

In general relativity, the equations describing the PK parameters in terms of the stellar masses are (see Damour & Deruelle 1986; Taylor & Weisberg 1989; Damour & Taylor 1992):

$$\dot{\omega} = 3 \left(\frac{P_b}{2\pi} \right)^{-5/3} (T_\odot M)^{2/3} (1 - e^2)^{-1} , \tag{16}$$

$$\gamma = e \left(\frac{P_b}{2\pi} \right)^{1/3} T_\odot^{2/3} M^{-4/3} m_2 (m_1 + 2m_2) , \tag{17}$$

$$\dot{P}_b = - \frac{192\pi}{5} \left(\frac{P_b}{2\pi} \right)^{-5/3} \left(1 + \frac{73}{24} e^2 + \frac{37}{96} e^4 \right) (1 - e^2)^{-7/2} T_\odot^{5/3} m_1 m_2 M^{-1/3} , \tag{18}$$

$$r = T_\odot m_2 , \tag{19}$$

$$s = x \left(\frac{P_b}{2\pi} \right)^{-2/3} T_\odot^{-1/3} M^{2/3} m_2^{-1} . \tag{20}$$

where $s \equiv \sin i$, $M = m_1 + m_2$ and $T_\odot \equiv GM_\odot/c^3 = 4.925490947\,\mu$s. Other theories of gravity, such as those with one or more scalar parameters in addition to a tensor component, will have somewhat different mass dependencies for these parameters.

A traditional method of comparing the observed results to the predictions of GR is through use of a "mass-mass" diagram such as that for PSR B1534+12 shown in Figure 2. This presents the 68% confidence regions for parameters measured using the theory-independent "DD" formalism, which makes no assumptions about the validity of any gravitational theory. If these curves intersect in a common region which includes the mass predictions based on GR, then the parameters may be said to agree with GR.

Weisberg & Taylor (in this volume) describe the excellent agreement of the observed parameters of PSR B1913+16 with GR. The slightly less eccentric system PSR B1534+12 allows detection of Shapiro delay in addition to the $\dot{\omega}$, $\dot{P}_\mathrm{b}$ and γ parameters measured for B1913+16, permitting an $\dot{\omega}$–γ–s combination which tests only the quasi-static regime of GR, an important complement to the "mixed" B1913+16 test (Stairs et al. 2002). The offset of $\dot{P}_\mathrm{b}$ for B1534+12 from its expected GR value can be attributed to a poorly known necessary kinematic correction due to the relative acceleration of the pulsar-system center-of-mass and Solar System Barycentre reference frames. The crucial unknown quantity is the distance to the pulsar. Under the assumption that GR is correct, the distance can be derived to be 1.04 ± 0.04 kpc (Stairs et al. unpublished), now among the most precisely measured pulsar distances.

New and unique constraints (notably that of the mass ratio) are of course available for the double-pulsar system (Lyne et al. 2004; articles by Kramer and others in this volume). Agreement with GR is also seen for $\dot{\omega}$, $\dot{P}_\mathrm{b}$ and γ (and the scintillation measurement of $\sin i$) in the pulsar–white-dwarf system PSR J1141−6545 (Bailes et al. 2003; Bailes, in the volume). The circular-orbit

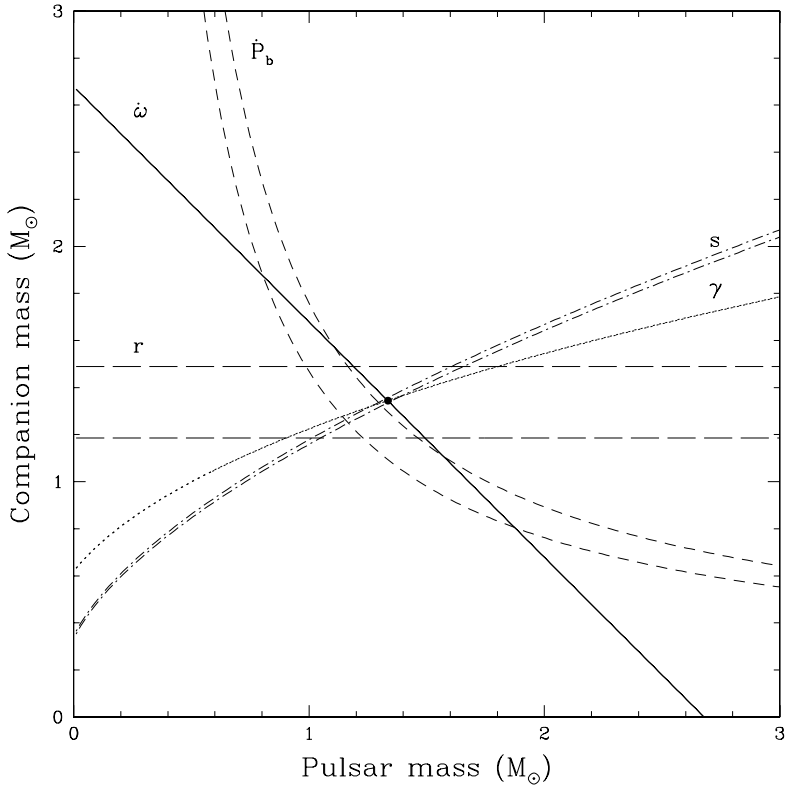

Figure 2. Mass-mass diagram for the PSR B1534+12 system. Labeled curves illustrate 68% confidence ranges of the DD parameters (Stairs et al. unpublished). The filled circle indicates the component masses according to the DDGR solution. The kinematic correction for assumed distance $d = 0.7 \pm 0.2\,\mathrm{kpc}$ (Taylor & Cordes 1993) has been subtracted from the observed value of $\dot{P}_b$; the uncertainty on this kinematic correction dominates the uncertainty of this curve. A slightly larger distance removes the small apparent discrepancy between the observed and predicted values of this parameter.

PSR–WD system J0437−4715 has a fully known orientation due to geometrical effects and the motions of the pulsar and the Earth (van Straten et al. 2001; Kopeikin 1995, 1996). The magnitude and shape of the Shapiro delay signal can be predicted based on the geometrically derived system inclination and compared to the predictions of GR; this results in an excellent match (van Straten et al. 2001). The same argument could be made for the wider-orbit PSR J1713+0747 for which the same angles have recently been measured (Splaver et al. 2005).

6. Geodetic Precession

The evolutionary scenarios for double-NS systems (e.g., Dewi & Pols 2003; Bethe & Brown 1998) predict that, immediately before the second supernova explosion,

the two stellar spin axes whould be aligned with the orbital angular momentum of the system. After the explosion, the recycled pulsar's spin axis direction should be unchanged, but the orbital angular momentum vector and most likely the spin axis of the companion will have changed direction. The resulting misalignment between the pulsar's spin axis and the orbital angular momentum vector will cause the former to precess around the latter. The evolution of the pulsar spin axis $\mathbf{S}_1$ can be written as (Damour & Ruffini 1974; Barker & O'Connell 1975b):

$$\frac{d\mathbf{S}_1}{dt} = \mathbf{\Omega}_1^{\rm spin} \times \mathbf{S}_1, \tag{21}$$

where the vector $\mathbf{\Omega}_1^{\rm spin}$ is aligned with the orbital angular momentum. Its magnitude is given by:

$$\Omega_1^{\rm spin} = \frac{1}{2}\left(\frac{P_{\rm b}}{2\pi}\right)^{-5/3} \frac{m_2(4m_1+3m_2)}{(1-e^2)(m_1+m_2)^{4/3}} T_\odot^{2/3}, \tag{22}$$

where again $T_\odot \equiv GM_\odot/c^3 = 4.925490947\,\mu$s. The predicted precession periods are roughly 700 years for PSR B1534+12, 300 years for PSR B1913+16, 270 years for PSR J1141−6545 and only 70–75 years for PSRs J0737−3039A and B. The primary manifestation of this precession is a slow change in the shape of the pulse profile, as different regions of the pulse emission beam move into the observable slice.

Weisberg & Taylor (in this volume) describe the profile shape changes and beam modeling of PSR B1913+16. While a range of possible beam models (Kramer 1998; Weisberg & Taylor 2002) point to a spin-orbit misalignment angle of about 20° and disappearance of the pulsar in about 20 years' time, there is significant uncertainty in the beam model itself, with both hourglass (Weisberg & Taylor 2002) and circular (Kramer 2002) models possible. This ambiguity has effectively prevented the observations from leading to a measurement of the precession rate independent of a beam model.

The situation is different for PSR B1534+12, which has stronger signal-to-noise in general and which has a polarization position angle swing that follows the rotating vector model (Radhakrishnan & Cooke 1969). In fact, for this pulsar, long-term changes are apparent in *both* the profile shape and the polarization properties. The polarization changes show that the impact parameter of the line of sight to the pulsar's magnetic pole is increasing in magnitude at a rate of about 0.2°/yr (Fig. 3). Under the assumption that this is due to geodetic precession of the spin axis, these changes provide an immediate insight into the 3-dimensional orientation of the pulsar's spin axis. Furthermore, the long-term evolution of the pulse profile shape can be modeled linearly and compared in magnitude to smaller but similar variations due to special-relativistic aberration on orbital timescales. Thus the unknown intrinsic pulse beam shape can be "calibrated out" and the precession rate measured (Stairs, Thorsett, & Arzoumanian 2004). While the rate measurement is still low-precision, it is in excellent agreement with the predictions of GR. Figures 3 and 4 show the profile and polarization changes, along with the aberration/precession measurement. Besides providing the first beam-model-independent test of the precession rate in strong-field gravity, these observations also yield the full 3-dimensional system

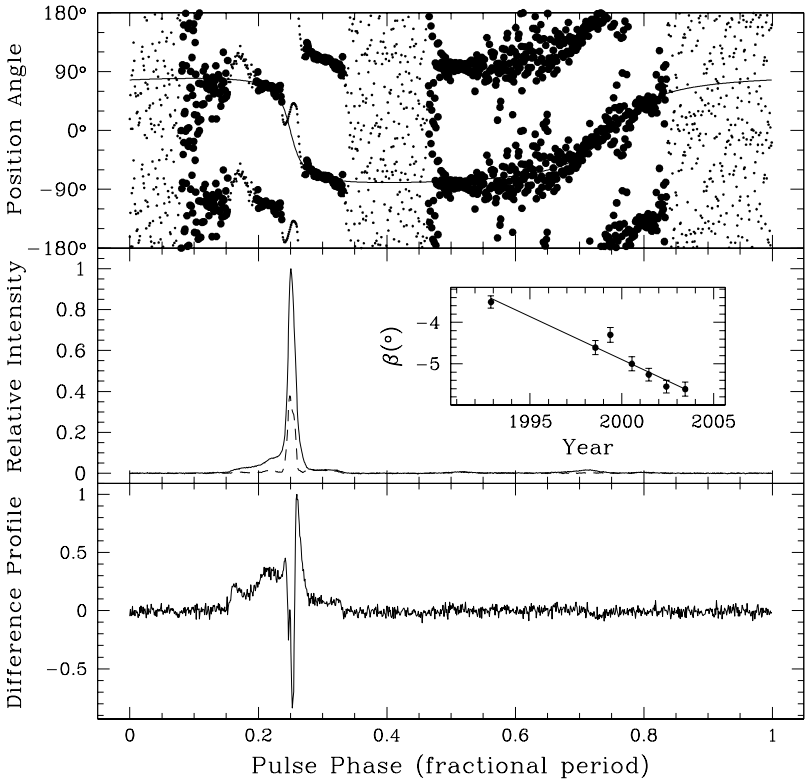

Figure 3. Top panel: the position angle of linear polarization in 2001 June, with best fit rotating vector model (RVM) overlaid. Only the position angle points indicated by large dots were used in the RVM fit; these were weighted by their uncertainties, with a small uncertainty added in quadrature to account for deviations from the RVM. Middle panel: total intensity (solid) and linear polarization (dashed) profiles in 2001 June. This profile is very similar in shape to our "reference" profile P_0. Inset: evolution of impact angle β with time. Bottom panel: "Difference" profile P_1, representing essentially the time-derivative of the observed profile. From Stairs, Thorsett & Arzoumanian (2004).

geometry for B1534+12, up to one ambiguity in the pair of angles representing the spin-orbit misalignment and the inclination angle of the system. The ambiguity can be resolved, and in fact the kick in the second supernova explosion can be tightly constrained, by tracing the pulsar's motion backwards in time through the Galaxy to plausible birth sites, allowing for a range of values in the unknown radial velocity. By combining the precession-derived geometry with the orbital orientation known from scintillation (Bogdanov et al. 2002), it can be shown that the immediate progenitor of the second neutron star was likely overflowing its Roche lobe, and that it received a kick of 230 ± 60 km/s (Thorsett, Dewey, & Stairs 2005; cf. Willems, Kalogera, & Henninger 2004).

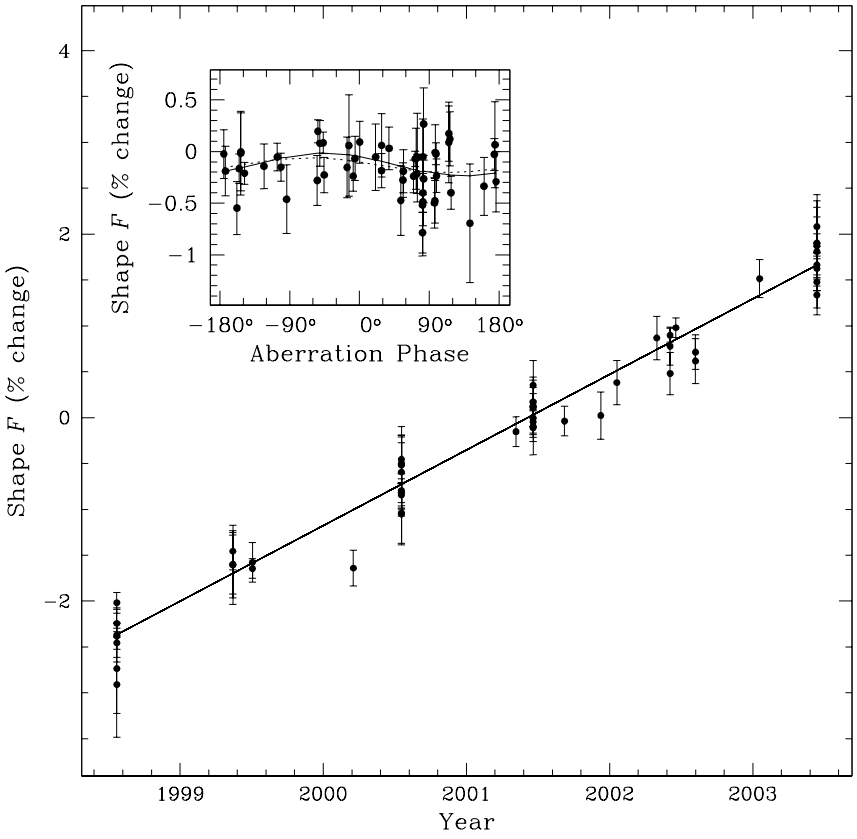

Figure 4. The ratio of the strengths of P_1 and P_0 for each observation is shown as a function of date in the main panel and aberration phase (essentially the true anomaly corrected for the advance of periastron) in the inset. The best-fit model is shown by the solid line in each panel, and in the orbital-phase plot, the GR prediction based on the RVM model is indicated by the dotted line. From Stairs, Thorsett & Arzoumanian (2004).

7. Conclusions

The next several years will be very exciting times for pulsars tests of GR, with new pulsars being discovered for equivalence-principle violation limits, potential for improving the precession rate test in PSR B1534+12 using wider-bandwidth observations, and the prospect of qualitatively new as well as unprecedentedly precise tests resulting from the double-pulsar system.

Acknowledgments. The author holds an NSERC UFA and is supported by a Discovery Grant. She thanks her collaborators on the J1713+0747 project: Eric Splaver, David Nice, Andrea Lommen and Don Backer, and the B1534+12 projects: Steve Thorsett, Zaven Arzoumanian and Rachel Dewey. She also thanks Michael Kramer and David Nice for helpful comments on the manuscript.

References

Arzoumanian, Z. 1995, PhD thesis, Princeton University

Arzoumanian, Z. 2003, in Bailes, M., Nice, D. J., & Thorsett, S. E., eds, Radio Pulsars. Astronomical Society of the Pacific, San Francisco, p. 69

Bailes, M., Ord, S. M., Knight, H. S., & Hotan, A. W. 2003, ApJ, 595, L49

Barker, B. M. & O'Connell, R. F. 1975a, Phys. Rev. D, 12, 329

Barker, B. M. & O'Connell, R. F. 1975b, ApJ, 199, L25

Bell, J. F. & Damour, T. 1996, Class. Quant. Grav., 13, 3121

Bell, J. F. 1996, ApJ, 462, 287

Bell, J. F., Camilo, F., & Damour, T. 1996, ApJ, 464, 857

Bethe, H. A. & Brown, G. E. 1998, ApJ, 506, 780

Bhattacharya, D. & van den Heuvel, E. P. J. 1991, Phys. Rep., 203, 1

Bogdanov, S., Pruszunska, M., Lewandowski, W., & Wolszczan, A. 2002, ApJ, 581, 495

Callanan, P. J., Garnavich, P. M., & Koester, D. 1998, MNRAS, 298, 207

Camilo, F., Nice, D. J., & Taylor, J. H. 1993, ApJ, 412, L37

Camilo, F., Nice, D. J., & Taylor, J. H. 1996, ApJ, 461, 812

Chandrasekhar, S. 1931, ApJ, 74, 81

Counselman, C. C. & Shapiro, I. I. 1968, Science, 162, 352

Damour, T. & Deruelle, N. 1986, Ann. Inst. H. Poincaré (Physique Théorique), 44, 263

Damour, T. & Esposito-Farèse, G. 1996, Phys. Rev. D, 53, 5541

Damour, T. & Esposito-Farèse. G. 1996b, Phys. Rev. D, 54, 1474

Damour, T. & Esposito-Farèse, G. 1992a, Phys. Rev. D, 46, 4128

Damour, T. & Esposito-Farèse, G. 1992b, 9, 2093

Damour, T. & Ruffini, R. 1974, C. R. Acad. Sc. Paris, Serie A, 279, 971

Damour, T. & Schäfer, G. 1991, Phys. Rev. Lett., 66, 2549

Damour, T. & Taylor, J. H. 1992, Phys. Rev. D, 45, 1840

Damour, T., Gibbons, G. W., & Taylor, J. H. 1988, Phys. Rev. Lett., 61, 1151

Dewi, J. D. M. & Pols 2003, MNRAS, 344, 629

Dickey, J. O. et al. 1994, Science, 265, 482

Eardley, D. M. 1975, ApJ, 196, L59

Esposito-Farese, G. 2003, in XXXVIII Rencontres de Moriond on Gravitational Waves and Experimental Gravity. The Gioi Publishers, p. 427

Gérard, J.-M. & Wiaux, Y. 2002, Phys. Rev. D, 66(24040), 1

Goldman, I. 1990, MNRAS, 244, 184

Hulse, R. A. & Taylor, J. H. 1975, ApJ, 195, L51

Kaspi, V. M. et al. 2000, ApJ, 543, 321

Kaspi, V. M., Taylor, J. H., & Ryba, M. 1994, ApJ, 428, 713

Konacki, M., Wolszczan, A., & Stairs, I. H. 2003, ApJ, 589, 495

Kopeikin, S. M. 1995, ApJ, 439, L5

Kopeikin, S. M. 1996, ApJ, 467, L93

Kramer, M. 1998, ApJ, 509, 856

Kramer, M. 2002, in IX Marcel Grossmann Meeting. World Scientific

Kuijken, K. & Gilmore, G. 1989, MNRAS, 239, 571

Lange, C., Camilo, F., Wex, N., Kramer, M., Backer, D., Lyne, A., & Doroshenko, O. 2001, MNRAS, 326, 274

Lightman, A. P. & Lee, D. L. 1973, Phys. Rev. D, 8, 3293

Lyne, A. G. et al. 2004, Science, 303, 1153

Ni, W. 1973, Phys. Rev. D, 7, 2880

Nice, D. J. & Taylor, J. H. 1995, ApJ, 441, 429

Nice, D. J., Taylor, J. H., & Fruchter, A. S. 1993, ApJ, 402, L49

Nordtvedt, K. & Will, C. M. 1972, ApJ, 177, 775

Nordtvedt, K. 1968, Phys. Rev., 170, 1186

Nordtvedt, K. 1990, Phys. Rev. Lett., 65, 953

Radhakrishnan, V. & Cooke, D. J. 1969, Astrophys. Lett., 3, 225

Rappaport, S., Podsiadlowski, P., Joss, P. C., DiStefano, R., & Han, Z. 1995, MNRAS, 273, 731

Reasenberg, R. D. 1983, Phil. Trans. Roy. Soc. A, 310, 227

Rosen, N. 1973, General Relativity and Gravitation, 4, 435

Shklovskii, I. S. 1970, Sov. Astron., 13, 562

Splaver, E. M., Nice, D. J., Stairs, I. H., Lommen, A. N., & Backer, D. C. 2005, ApJ, in press, astro-ph/0410488

Stairs, I. H. 2003, Living Reviews in Relativity, 6, 5

Stairs, I. H., Thorsett, S. E., Taylor, J. H., & Wolszczan, A. 2002, ApJ, 581, 501

Stairs, I. H., Thorsett, S. E., & Arzoumanian, Z. 2004, Phys. Rev. Lett., 93, 141101

Taylor, J. H. & Cordes, J. M. 1993, ApJ, 411, 674

Taylor, J. H. & Weisberg, J. M. 1989, ApJ, 345, 434

Thorsett, S. E. & Chakrabarty, D. 1999, ApJ, 512, 288

Thorsett, S. E. 1996, Phys. Rev. Lett., 77, 1432

Thorsett, S. E., Dewey, R. J., & Stairs, I. H. 2005, ApJ, in press, astro-ph/0408458

Toscano, M., Sandhu, J. S., Bailes, M., Manchester, R. N., Britton, M. C., Kulkarni, S. R., Anderson, S. B., & Stappers, B. W. 1999, MNRAS, 307, 925

van Straten, W., Bailes, M., Britton, M., Kulkarni, S. R., Anderson, S. B., Manchester, R. N., & Sarkissian, J. 2001, Nature, 412, 158

Wagoner, R. V. 1975, ApJ, 196, L63

Weisberg, J. M. & Taylor, J. H. 1981, General Relativity and Gravitation, 13, 1

Weisberg, J. M. & Taylor, J. H. 2002, ApJ, 576, 942

Wex, N. 1997, A&A, 317, 976

Wex, N. 2000, in Kramer, M., Wex, N., Wielebinski, R., eds, Pulsar Astronomy - 2000 and Beyond, IAU Colloquium 177. Astronomical Society of the Pacific, San Francisco, p. 113

Will, C. M. & Nordtvedt, K. J. 1972, ApJ, 177, 757

Will, C. M. 1992, ApJ, 393, L59

Will, C. M. 1993, Theory and Experiment in Gravitational Physics. Cambridge University Press, Cambridge

Will, C. 2001, Living Reviews in Relativity, 4, 4

Willems, B., Kalogera, V., & Henninger, M. 2004, ApJ, 616, 414